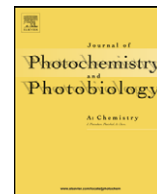




Contents lists available at ScienceDirect

# Journal of Photochemistry and Photobiology A: Chemistry

journal homepage: [www.elsevier.com/locate/jphotochem](http://www.elsevier.com/locate/jphotochem)

## Nonlinear instabilities in the light-mediated bromate–4-aminophenol reaction

Mohammad Harati, Sheida Amiralaie, James R. Green\*, Jichang Wang\*

Department of Chemistry and Biochemistry, University of Windsor, Ontario N9B 3P4, Canada

### ARTICLE INFO

#### Article history:

Received 24 October 2007

Received in revised form 20 February 2008

Accepted 25 February 2008

Available online 29 February 2008

#### Keywords:

Nonlinear dynamics  
Chemical oscillations  
Photochemistry  
Spectroscopy

### ABSTRACT

The kinetics and mechanism of the photo-illuminated bromate–4-aminophenol (AP) reaction were investigated in this report, in which chemical oscillations were observed over broad reaction conditions when the applied light intensity was above a threshold level. Besides Pt and bromide potentials, absorption spectra also exhibit large amplitude oscillations within a wavelength between 300 and 440 nm. Phase diagrams in a three-dimensional concentration space illustrate that the oscillatory behaviour is more sensitive to the ratio of  $[AP]/[BrO_3^-]$  than their actual concentrations. The induction time and number of oscillations show different dependence on the concentrations of the initial reactants. Several intermediates were identified by mass spectrometry,  $^1H$  NMR and  $^{13}C$  NMR methods, and possible mechanisms leading to the formation of those intermediates were discussed.

© 2008 Elsevier B.V. All rights reserved.

### 1. Introduction

Behaviour of an oscillatory reaction system can be conveniently manipulated through varying external parameters such as the flow rate in a continuous flow stirred tank reactor (CSTR), the concentration of a reagent, or, light illumination if the system is photosensitive [1–10]. Perhaps the most beautiful instance of such a controlling influence is the stabilization of unstable limit cycle oscillations in a chaotic Belousov-Zhabotinsky (BZ) system through perturbing the flow rate at which the metal catalyst and bromate solutions are fed into a CSTR [11]. From a practical point of view, using light as the control parameter has great advantages due to the easy regulation of both intensity and illumination protocols, particularly in the study of reaction-diffusion media in which spatially inhomogeneous perturbations are sometimes desired. As a result, photosensitive chemical oscillators have attracted a great deal of attention in the past three decades [12–28].

Based on the function of light in the studied systems, photochemical oscillators can be loosely classified into two groups, namely photosensitive oscillators and photo-controlled oscillators. For photosensitive chemical systems, illumination merely provides an alternative approach of producing key intermediates and the vast majority of existing investigations on nonlinear photochemical dynamics have been carried out in this category [12–24]. In the ruthenium-catalyzed BZ reaction, for example, light causes additional production of bromide ions, an inhibitor of the autocatalytic

reaction [19]. Vanag and Hanazaki studied the photosensitivity of the ferroin-catalyzed BZ reaction in the water-in-oil microemulsion system [20]. Extensive studies on the effect of light on the Bray reaction were performed by Noyes and co-workers [21,22]. Subtle photosensitive behaviour has been observed in both the uncatalyzed and catalyzed bromate–1,4-cyclohexanedione reaction (CHD), in which the response of the reaction to light does not only depend on the compositions of the system but also depends on the light intensity [23,24].

For photo-controlled chemical reactions, light creates an exclusive approach of producing certain intermediates. Therefore, the system does not exhibit any reactivity in the absence of illumination [25–31]. Examples of those systems include the photo-degradation of tetrathionate, and the photo-mediated bromate–1,4-benzoquinone reactions [25–27]. In a recent letter [28], we reported that the bromate–4-aminophenol (AP) reaction also belongs to the group of photo-controlled chemical oscillators, in which significant reactivity, especially chemical oscillations, could be achieved only in the presence of light. In the following, the kinetics and mechanism of the photo-mediated bromate–AP reaction were systematically investigated and characterized with different analytical methods.

### 2. Experimental

All reactions were carried out in a thermal-jacketed 50 ml glass beaker purchased from ChemGlass and temperature was kept at  $25.0 \pm 0.1$  °C by a circulating water bath (Thermo NesLab RTE 7). Reactions were monitored with a platinum electrode coupled with a  $Hg|Hg_2SO_4|K_2SO_4$  reference electrode (Radiometer Analytical). All measurements were recorded through a pH/potential meter

\* Corresponding authors. Fax: +1 519 973 7089.  
E-mail addresses: [jgreen@uwindsor.ca](mailto:jgreen@uwindsor.ca) (J.R. Green),  
[jwang@uwindsor.ca](mailto:jwang@uwindsor.ca) (J. Wang).

(Radiometer PHM220) connected to a personal computer through a PowerLab/4SP data logger. A halogen lamp with dual bifurcated optic fibers and continuous variable light level was used as the light source (Fisher Scientific, Model DLS-100HD, 150 W).

Mass spectrometry studies were performed with a 1200 L single quadrupole MS (Varian) using a direct insertion probe. The mass range was between 10 and 800 amu and electron ionization was used as ionization mode. The probe temperature was controlled independently and changed from 20 to 300 °C with the same steps and durations for all the MS measurements. The samples have been prepared as follows: the reaction was stopped at different stages by adding 30 ml diethyl ether ( $\geq 99.0\%$ , purchased from Sigma–Aldrich) to the reaction mixture and subsequently separating the organic phase. The remaining aqueous phase was then extracted twice, respectively, with 30 ml diethyl ether. Later, a rotary evaporator was used to concentrate the diethyl ether sample, which took about 60 min. The mass spectra of all samples were recorded at 20 eV electron impact. All  $^1\text{H}$  NMR and  $^{13}\text{C}$  NMR measurements were carried out using Bruker Avance 500 MHz spectrometer and with the same sample that was used for mass spectrometry studies but dissolved in chloroform- $d$  (99.8%) or acetone- $d_6$  (99.9%) purchased from Cambridge Isotope Laboratories.

Stock solutions of  $\text{NaBrO}_3$  (Aldrich, 99%), 0.6 M, and sulfuric acid (Aldrich, 95–98%), 4.0 M, were prepared with double-distilled water. 4-Aminophenol (Aldrich, >98%) was directly dissolved in the reaction mixture. The volume of the reaction mixture was kept at 30.0 ml in all experiments. Absorption spectra were measured with a UV–visible spectrophotometer from Ocean Optics (2000 USB), in which a quartz cuvette (10 mm light path, HELMA) containing 2.5 ml sample mixture was placed in a CUV sample holder which has two water jackets connected to a circulating water bath (Thermo NesLab RTE 7). The cuvette was stirred with a small magnetic bar.

### 3. Results and discussion

Fig. 1 shows the temporal evolution of the illuminated bromate–AP reaction under different initial concentrations of AP: (a) 0.011 M, (b) 0.018 M, and (c) 0.029 M. In all three cases, the reaction evolves through a broad peak in the Pt potential, which is

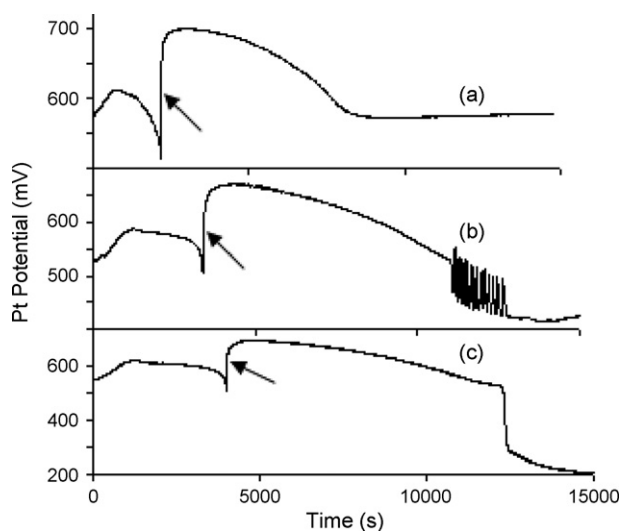


**Fig. 1.** Time series of the illuminated bromate–AP reaction under different concentrations of AP: (a) 0.011 M, (b) 0.018 M, and (c) 0.029 M. Other reaction conditions are:  $[\text{BrO}_3^-] = 0.050 \text{ M}$ ,  $[\text{H}_2\text{SO}_4] = 1.70 \text{ M}$ , and light intensity =  $100 \text{ mW/cm}^2$ .

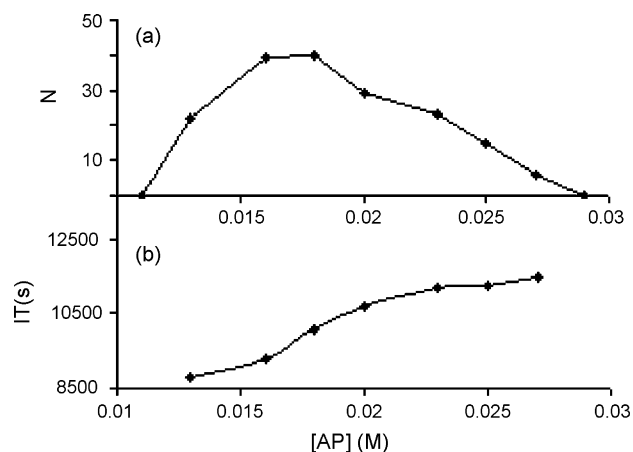


**Fig. 2.** Dependence of the induction time (IT) and number of oscillations on the concentration of AP. Other reaction conditions are the same as those used in Fig. 1.

followed by an abrupt potential increase as indicated by the arrows. Depending on the compositions of the reaction, yellow precipitates may occur during the first broad peak, but disappear rapidly and completely by the occurrence of the sharp Pt potential increase. Beyond this point, the evolution of the reaction system becomes qualitatively different from (a) to (c). At the low AP concentration, the Pt potential decreases smoothly in time until a constant value is achieved at about 3 h after mixing all reagents together. Under a moderate AP concentration, however, periodic oscillations in the Pt potential take place. Notably, there is a long induction time before the spontaneous chemical oscillations occur. When the concentration of AP is too high, the smooth decrease of the Pt potential is interrupted by a sudden decrease at about 10,000 s after the reaction has begun, but no oscillation takes place afterwards. This figure illustrates that, in addition to an above threshold light intensity [28], AP concentration must be within a proper range for this photochemical system to exhibit oscillatory behaviour.

Fig. 2 plots the variation of the induction time and number of oscillations as a function of AP concentration. Under the conditions studied here, chemical oscillations have been found within the range between 0.013 and 0.027 M. Fig. 2a illustrates that, as the concentration of AP is gradually increased, the total number of oscillations first increases, reaching a maximum of 40 peaks, and then decreases gradually until the system moves out of the oscillation window. On the other hand, as is shown in Fig. 2b, the induction time increases monotonically with the concentration of AP, indicating that the induction time is not related to the number of oscillation peaks.

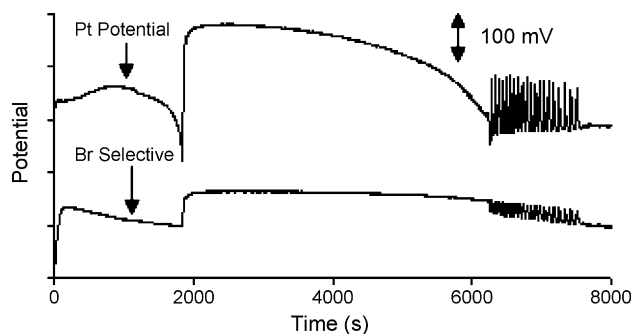


**Fig. 3.** Time series recorded simultaneously with a bromide ion selective electrode and a Pt electrode. The reaction conditions are  $[\text{BrO}_3^-] = 0.050 \text{ M}$ ,  $[\text{H}_2\text{SO}_4] = 1.70 \text{ M}$ ,  $[\text{AP}] = 0.020 \text{ M}$ , and light intensity =  $150 \text{ mW/cm}^2$ .

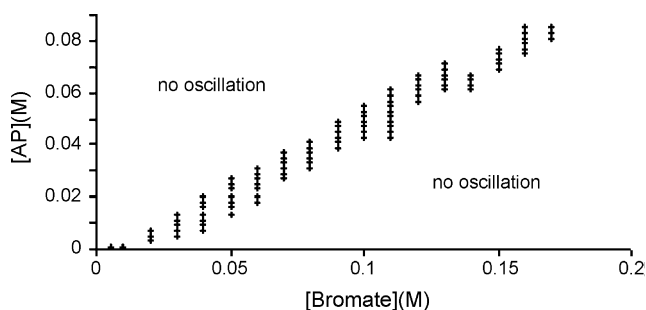


Fig. 4. Phase diagram in the AP–bromate concentration plane. (◆) Indicates the conditions under which the system shows spontaneous oscillations. Other reaction conditions are  $[\text{H}_2\text{SO}_4] = 1.70 \text{ M}$  and light intensity is  $100 \text{ mW/cm}^2$ .

Fig. 3 presents the evolution of the illuminated bromate–AP reaction recorded simultaneously with a bromide selective electrode and a Pt electrode. In bromate-based chemical oscillators,  $\text{Br}^-$  plays a critical role via rapidly reacting with the autocatalyst  $\text{HBrO}_2$  [32,33]. As shown in this figure, the abrupt increase in the Pt potential coincides with an abrupt increase of the bromide potential. The calibration shows that high bromide electrode potential corresponds to low bromide concentration. The sudden disappearance of the yellow precipitate thus accompanies a sudden decrease of bromide concentration. Such a dramatic process may arise from an autocatalytic production of  $\text{HBrO}_2$ , which consequently consumes bromide via the reaction  $\text{HBrO}_2 + \text{Br}^- + \text{H}^+ \rightarrow 2\text{HOBr}$ . The above measurement also shows that bromide concentration increases slowly during the long induction time and then oscillates toward a higher value. Due to that bromide electrode is sensitive to illumination, only a few reactions were recorded simultaneously with the Pt and bromide selective electrodes.

Fig. 4 presents a phase diagram in a bromate and AP concentration plane, where (◆) indicates the conditions under which the system exhibits spontaneous oscillations. At first glance, Fig. 4 suggests that the illuminated bromate–AP system is able to oscillate over a broad concentration range of AP and bromate; however, at a fixed concentration of AP (or bromate), the suitable concentration range of bromate (or AP) is quite narrow. The diagonal-structured parameter window suggests that the reaction behaviour is more sensitive to the ratio of  $[\text{bromate}]/[\text{AP}]$  than their actual concentrations. Moreover, this phase diagram illustrates that increasing AP concentration shifts the suitable bromate concentration toward higher values. An useful note is that when the bromate concentration is higher than  $0.08 \text{ M}$ , the system evolves into the oscillatory window through one process, where the yellow precipitates disappear gradually and thus there are no sudden increases in the Pt and bromide potentials as seen in Fig. 3.

The studied system involves three reactants, namely bromate, 4-aminophenol and acid. Determining the oscillation parameter window in a three-dimensional concentration space represents a tremendous challenge as a huge number of experiments would be required. To partially overcome such a challenge and gain some meaningful insight into the reaction behaviour in a three-dimensional parameter space, Fig. 5 presents a primitive three-dimensional phase diagram which was constructed by establishing phase diagrams in the bromate–AP plane at two concentrations of acid. This primitive 3D plot indicates that the parameter window within which the system exhibits spontaneous oscillations is a thin slab in the bromate–acid–AP concentration space, implicating that nonlinear behaviour in the studied system is more sensitive to the ratio of  $[\text{AP}]/[\text{bromate}]$  than their absolute concentrations.

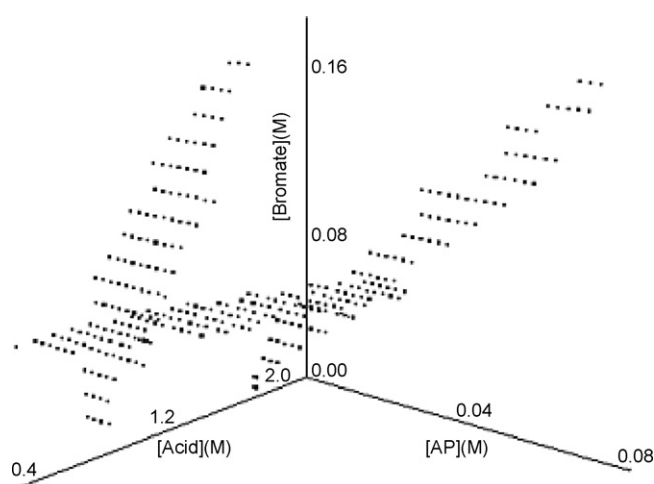


Fig. 5. Phase diagram in a three-dimensional concentration space. (◆) Indicates the conditions under which the system exhibits spontaneous oscillations. The light intensity is  $100 \text{ mW/cm}^2$ .

Our experiments illustrate that the dependence of the number of oscillations on bromate concentration is similar to what was obtained when AP concentration was adjusted, suggesting that bromate has similar effects as AP on the oscillatory behaviour. Despite there being an optimum concentration for the largest number of oscillations, the induction time nevertheless increases monotonically with respect to bromate concentration. The study on the influences of acid concentration on the oscillatory behaviour shows that, different from the cases of bromate and aminophenol, the induction time does not exhibit significant change when the acid concentration is adjusted. For both acid and bromate, there is a rapid increase in the induction time when the system moves closer to the upper threshold concentration of the acid or bromate.

It has been reported in the earlier letter that the applied light intensity must be above a threshold value for the system to exhibit significant reactivity, in particular the oscillatory behaviour [28]. The effect of light intensity on the number of oscillations is presented here in Fig. 6. In this series of experiments, there is no oscillatory phenomenon when the applied light intensity is lower than  $30 \text{ mW/cm}^2$ . Above such a critical value, the number of peaks increases gradually with the light intensity. Beyond  $90 \text{ mW/cm}^2$ , however, further increase of light intensity exhibits adverse influences on the oscillatory behaviour, causing a decrease in the number of oscillations. Within the above parameter window, the amplitude of oscillation increases monotonically while the induction time decreases monotonically with increasing light intensity. Limited by the light source, we have not been able to reach the

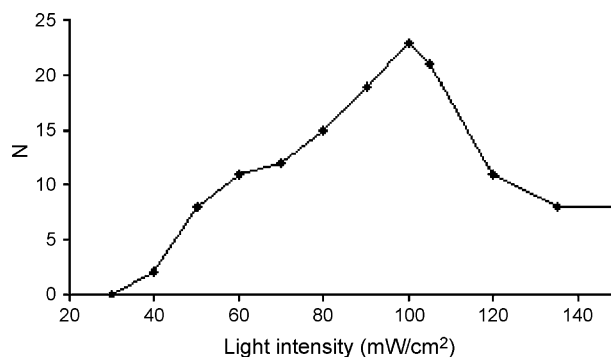
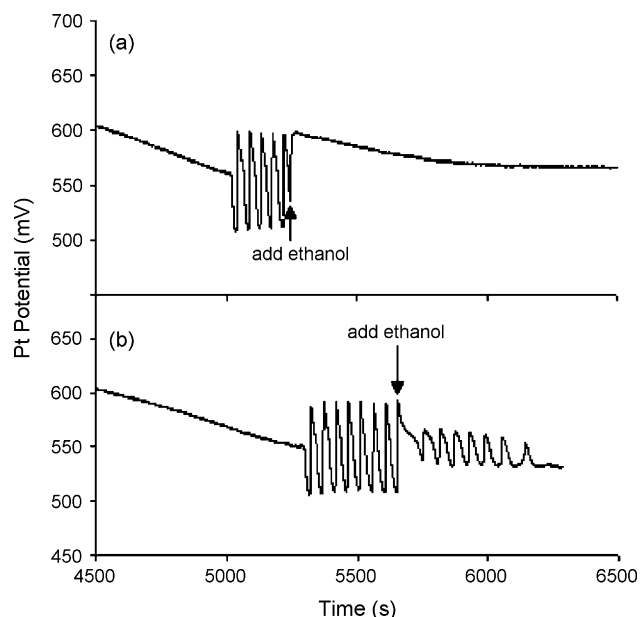


Fig. 6. Dependence of the number of oscillations on light intensity. Other reaction conditions are  $[\text{H}_2\text{SO}_4] = 1.70 \text{ M}$ ,  $[\text{BrO}_3^-] = 0.050 \text{ M}$ , and  $[\text{AP}] = 0.023 \text{ M}$ .



**Fig. 7.** Quenching behaviour with the addition of ethanol: (a)  $4 \times 10^{-3}$  M, and (b)  $1 \times 10^{-3}$  M. Other reaction conditions are  $[\text{H}_2\text{SO}_4] = 1.70$  M,  $[\text{BrO}_3^-] = 0.050$  M,  $[\text{AP}] = 0.016$  M, and light intensity =  $150 \text{ mW/cm}^2$ .

upper limit of the light intensity beyond which the system does not oscillate.

The inhibitory effect of aliphatic alcohols on bromate-based chemical oscillators such as the BZ reaction has been reported earlier, in which when small amounts of ethanol were added to an oscillating mixture, the oscillations became strongly damped and after some time the oscillation terminated [34–36]. Fig. 7 presents the influence of ethanol on the illuminated bromate–AP reaction, where the addition of  $4.0 \times 10^{-3}$  M of ethanol immediately quenches the oscillatory behaviour, whereas the oscillation amplitude is significantly reduced by  $1.0 \times 10^{-3}$  M ethanol. Different from the response to bromide ion perturbation, here the impact of ethanol is irreversible, implying that ethanol is not consumed like bromide ions. Studies with a UV/vis absorption method (at 330 nm) show that ethanol reacts with acidic bromate to produce HOBr, which can act as a radical scavenger through reacting with organic radicals or can directly interact with bromide ions to affect the reaction dynamics. In Fig. 7a, the addition of ethanol causes an immediate increase of the Pt potential, which corresponds to a decrease of bromide concentration as illustrated in Fig. 3. It thus suggests that the above-observed inhibitory effect of ethanol arises from the production of HOBr, which subsequently consumes bromide ions.

Fig. 8 plots the amplitude of oscillations measured with a UV/vis spectrophotometer at different wavelengths. The result shows that intermediates which have strong absorptions within the wavelength between 310 and 430 nm oscillate in time. Known species which have strong absorption within such a range include HOBr (330 nm),  $\text{Br}_2$  (390 nm), *N*-bromo-1,4-benzoquinone-4-imine (250 and 330 nm). No oscillation was achieved when the evolution was followed at other wavelengths, despite the fact that the reaction solution, especially AP, has strong absorption within the UV range.

To decipher the mechanism of this illuminated bromate–AP reaction, mass spectrometry (electron impact, direct insertion) and  $^1\text{H}$  NMR analysis were performed at different reaction stages denoted respectively by 1–3 in Table 1. In the earlier work [28], we have identified that *N*-bromo-1,4-benzoquinone-4-imine, which is referred to as imine hereafter, is the precipitate formed at the

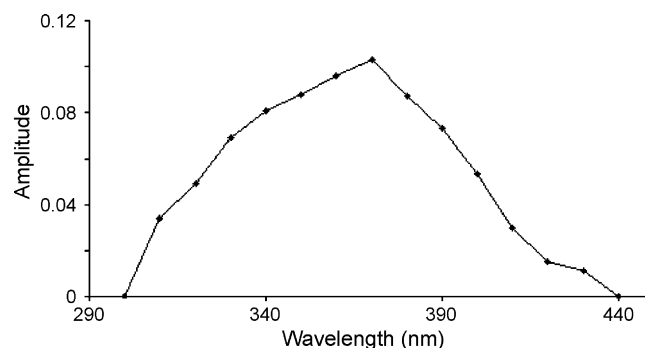


**Fig. 8.** The largest amplitude of oscillation measured with a UV/vis spectrophotometer at different wavelengths. Reaction conditions are:  $[\text{AP}] = 0.023$  M,  $[\text{H}_2\text{SO}_4] = 1.70$  M,  $[\text{BrO}_3^-] = 0.05$  M, and light intensity =  $150 \text{ mW/cm}^2$ . The spectra were taken by placing a 2.5 ml solution which just started oscillating in a regular reactor into a stirred 1.0 cm path length cuvette. The cuvette was then illuminated with  $50 \text{ mW/cm}^2$  light along a vertical direction.

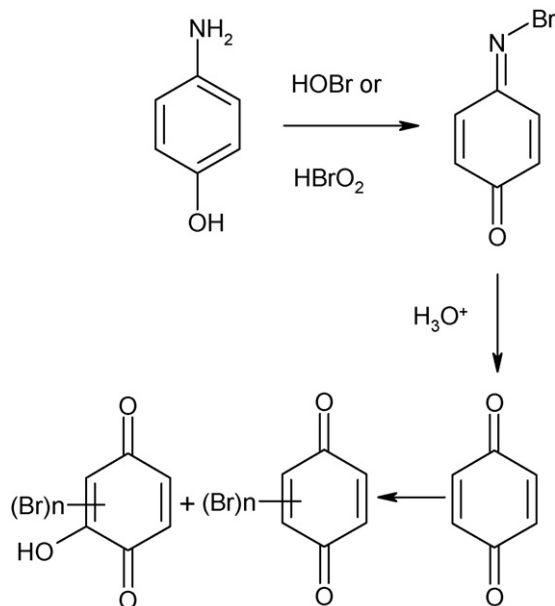
beginning of the reaction. Therefore, before spontaneous oscillations commence there are at least two stable organic compounds in the reaction mixture, namely AP and imine. The sample was analysed when the reaction was stopped at about 300 s after mixing all reagents together (i.e. stage 1). To carry out the analysis, the reaction mixture was first filtered to remove imine precipitate and then was extracted with diethyl ether solvent. The extracted solvent was analysed with the NMR and mass spectroscopy. The second reaction stage is when the yellow imine precipitate has completely dissolved but the oscillation has yet to appear (ca. 7000 s after mixing all reagents together). Again, the reaction was stopped by adding diethyl ether into the solution. The third stage is when the system starts oscillating. In both of the subsequent stages, the reaction was stopped by adding diethyl ether to the solution and analysed.

Using the same samples for each technique, mass spectra and  $^1\text{H}$  NMR spectra were acquired, and at each stage show many peaks that make them impossible to interpret completely. However, in  $\text{CDCl}_3$  solution we could assign the resonance at 6.78 ppm to 1,4-benzoquinone (1,4-BQ), which is the dominant species in solution at stage 1. The  $^{13}\text{C}$  NMR spectrum shows two peaks at 138 ppm and 187 ppm that belong to 1,4-BQ [37], and such a conclusion is further supported by DEPT-135 experiments. The mass spectral data in addition indicate monobrominated molecules of  $m/e$  186/188 and 188/190 and dibrominated species centred at  $m/e$  266 and 268. By stage 2, the  $^1\text{H}$  NMR spectrum ( $\text{CDCl}_3$ ) displays resonances at 6.82 and 6.94 ppm (each, doublet  $J = 10.3$  Hz) in addition to 1,4-benzoquinone, which are consistent with the presence of a 2,3-unsymmetrically disubstituted quinone, of which we consider 2-bromo-3-hydroxy-1,4-benzoquinone a most likely candidate.  $^1\text{H}$  NMR spectroscopy in acetone- $d_6$  gives a greater spectral separa-

**Table 1**  
Proposed chemical species on the basis of mass spectra

Reaction stage	Mass ( $m/e$ )	Suggested species
1 and 2	186/188	(O) $\text{C}_6\text{H}_3\text{Br}(\text{O})$
1 and 2	188/190	(OH) $\text{C}_6\text{H}_3\text{Br}(\text{HO})$
1 and 2	264/266/268	(O) $\text{C}_6\text{H}_2\text{Br}_2(\text{O})$
1–3	266/268/270	(OH) $\text{C}_6\text{H}_2\text{Br}_2(\text{H}_2\text{O})$
1–3	282/284/286	(OH) $_2\text{C}_6\text{H}_2\text{Br}_2(\text{HO})$
2 and 3	280/282/284	(O) $\text{C}_6\text{H}_2\text{Br}_2\text{OH}(\text{O})$
2	234/236/238	$\text{C}_6\text{H}_4\text{Br}_2$
2	141	(OH) $_3\text{C}_6\text{H}_2(\text{H}_2\text{N})$
2	342/344/346/348	(O) $\text{C}_6\text{HBr}_3(\text{O})$
2	344/346/348/350	(OH) $\text{C}_6\text{HBr}_3(\text{OH})$
1 and 2	108	$\text{OC}_6\text{H}_4\text{O}$
2 and 3	202/204	(O) $\text{C}_6\text{H}_3\text{BrOH}(\text{O})$





**Scheme 1.** Proposed dominant reaction pathway.

tion of the components, and reveals the presence of additional resonances consistent with the presence of additional substituted, and likely brominated, quinones. In the <sup>13</sup>C NMR spectrum, additional resonances in the 180–190 ppm region are indicative of the additional quinones. The mass spectral studies indicate the continued presence of the 186/188, 188/190, 266 and 268 ions, the 202/204 ions consistent with 2-bromo-3-hydroxy-1,4-benzoquinone, the appearance of a dibromo-monohydroxylated species centred at *m/e* 282, and trace amounts of tribrominated ions at 342/344/346/348 and 344/346/348/350; in conjunction with the NMR spectral data, we view these species as most likely quinones and hydroquinones, as opposed to protonated quinone imines and aminophenols. By stage 3, the purported 2-

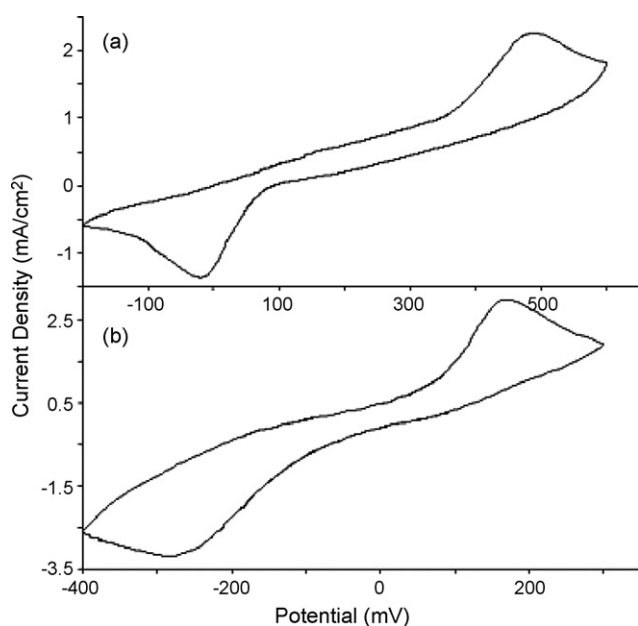


**Fig. 9.** Cyclic voltammograms of the (a) AP and (b) imine solution. The measurements were conducted by dissolving 0.023 M AP or imine in a 1.0 M H<sub>2</sub>SO<sub>4</sub> solution. The scanning rate is 50 mV/s.

bromo-3-hydroxy-1,4-benzoquinone (*m/e* 202/204) is significant, but most of the same species as stage 2 are present, by both <sup>1</sup>H NMR spectroscopy and mass spectroscopy. The dominant reaction route appears to involve oxidation of the 4-aminophenol to *N*-bromobenzoquinone imine, acidic imine hydrolysis to benzoquinone, and subsequent bromination and hydroxybromination reactions of the 1,4-BQ (Scheme 1).

Mechanistic studies with the cyclic voltammetry method show that the redox potential of 4-aminophenol is 235 mV vs. Hg|Hg<sub>2</sub>SO<sub>4</sub>|K<sub>2</sub>SO<sub>4</sub> electrode, whereas the redox potential of the intermediate imine is -52.5 mV against the same reference electrode (see Fig. 9). Such a result suggests that the intermediate reagent, imine, is a better reducing agent than the initial reactant AP and shall be easily oxidized further once formed. As discussed above and listed in Table 1, both mono- and di-bromated organic substances are produced in the reaction process. The bromination could take place through the organic substrates reacting with bromine or HOBr. It is worthwhile to mention that HOBr can act as: (1) a bromination agent [38]; (2) an oxidation agent [39]; and (3) a hydroxylation reactant [40–42]. The OKN mechanism has discussed how HOBr acts as a hydroxylation agent [40–42]. The production of 1,4-benzoquinone (1,4-BQ) could happen via the reaction of imine with H<sub>2</sub>O in an acidic environment, which is a well-known process [43]. Separate mass spectrometry analysis confirms that bromine reacts with 4-aminophenol producing (O)C<sub>6</sub>H<sub>4</sub>(NBr) in acidic solution.

#### 4. Conclusions

This study investigated the kinetics and mechanism of the light-mediated bromate–4-aminophenol reaction and showed that chemical oscillations in the studied system exist over broad concentration ranges of bromate, 4-aminophenol and sulfuric acid. However, as illustrated by the phase diagrams in a three-dimensional concentration space, the oscillatory behaviour is more susceptible to the ratio of [BrO<sub>3</sub><sup>-</sup>]/[AP] than their actual concentrations. Within the parameter regime where the system oscillates, increasing the concentration of bromate or AP shows the same kind of influence on the induction time and the number of oscillations as increasing the applied light intensity.

Quenching experiments suggest that the bromate–AP photochemical oscillator is bromide-controlled. Therefore, the autocatalytic production of HBrO<sub>2</sub> through the reduction of bromine dioxide radicals by organic substrates could still be responsible here for the nonlinear feedbacks, similar to the bromate-based chemical oscillators reported earlier [24,26,33]. Meanwhile, this photochemical oscillator can also be controlled by ethanol, which reacts with acidic bromate to produce HOBr, an intermediate which reacts with bromide ions [41] and acts as a radical scavenger to remove organic radicals [6]. Several intermediates are identified in this report with mass spectrometry, and NMR methods. The detection of small amounts of hydroquinones suggests the occurrence of photoreductions of the quinones [29]. These results should greatly facilitate the further investigations on the bromate–aromatic compounds reactions, which have exhibited both subtle photosensitivity and interesting reaction dynamics.

#### Acknowledgements

The authors would like to thank financial support from National Science and Engineering Research Council (NSERC), Canada, and Canada Foundation for Innovation (CFI).

## References

- [1] R.J. Field, M. Burger (Eds.), *Oscillations and Traveling Waves in Chemical Systems*, Wiley-Interscience, New York, 1985.
- [2] S.K. Scott, *Chemical Chaos*, Oxford University Press, 1994.
- [3] I.R. Epstein, J.A. Pojman, *An Introduction to Nonlinear Chemical Dynamics*, Oxford University Press, New York, 1998.
- [4] J. Wang, P.G. Sorensen, F. Hynne, *J. Phys. Chem.* 98 (1994) 725–727.
- [5] G. Schmitz, L. Kolar-Anic, S. Anic, T. Grozdic, V. Vukojevic, *J. Phys. Chem. A* 110 (2006) 10361–10368.
- [6] P.I. Kumli, M. Burger, M.J.B. Hauser, S.C. Müller, Z. Nagy-Ungvarai, *Phys. Chem. Chem. Phys.* 5 (2003) 5454–5458.
- [7] J.L. Hudson, M. Hart, D. Marinko, *J. Chem. Phys.* 71 (1979) 1601–1606.
- [8] R.H. Simoyi, A. Wolf, H.L. Swinney, *Phys. Rev. Lett.* 49 (1982) 245–248.
- [9] M. Dolnik, I. Schreiber, M. Marek, *Phys. Lett. A* 100 (1984) 316–319.
- [10] R. Blittersdorf, A.F. Munster, F.W. Schneider, *J. Phys. Chem.* 96 (1992) 5893–5897.
- [11] V. Petrov, V. Gaspar, J. Masere, K. Showalter, *Nature* 361 (1993) 240–243.
- [12] G. Rábai, I. Hanazaki, *J. Phys. Chem.* 98 (1994) 10550–10553.
- [13] V. Gaspar, G. Bazsa, M.T. Beck, *Z. Phys. Chem. Leipzig* 264 (1983) 43–48.
- [14] S. Kéki, G. Székely, M.T. Beck, *J. Phys. Chem. A* 107 (2003) 73–75.
- [15] J.R. Bamforth, J.H. Merkin, S.K. Scott, R. Toth, V. Gáspár, *Phys. Chem. Chem. Phys.* 3 (2001) 1435–1438.
- [16] S. Kadar, J. Wang, K. Showalter, *Nature* 391 (1998) 770–772.
- [17] O. Steinbock, V. Zykov, S.C. Müller, *Nature* 366 (1993) 322–324.
- [18] S.L. Kuhnert, K.I. Agladze, V.I. Krinsky, *Nature* 337 (1989) 244–247.
- [19] S. Kadar, T. Amemiya, K. Showalter, *J. Phys. Chem. A* 101 (1997) 8200–8206.
- [20] V.K. Vanag, I. Hanazaki, *J. Phys. Chem. A* 101 (1997) 2147–2152.
- [21] K.R. Sharma, R.M. Noyes, *J. Am. Chem. Soc.* 98 (1976) 4345–4361.
- [22] J.A. Odutola, C.A. Bohlander, R.M. Noyes, *J. Phys. Chem.* 86 (1982) 818–824.
- [23] D.S. Huh, H.S. Kim, J.K. Kang, Y.J. Kim, D.H. Kim, S.H. Park, K. Yadav, J. Wang, *Chem. Phys. Lett.* 378 (2003) 78–84.
- [24] J. Wang, K. Yadav, B. Zhao, Q. Gao, D. Huh, *J. Chem. Phys.* 121 (2004) 10138–10144.
- [25] A.K. Horváth, I. Nagypál, I.R. Epstein, *J. Am. Chem. Soc.* 124 (2002) 10956–10957.
- [26] B. Zhao, J. Wang, *Chem. Phys. Lett.* 430 (2006) 41–44.
- [27] B. Zhao, J. Wang, *J. Photochem. Photobiol. A: Chem.* 192 (2007) 204–210.
- [28] M. Harati, S. Amiralaei, J. Green, J. Wang, *Chem. Phys. Lett.* 439 (2007) 337–341.
- [29] H. Görner, *Photochem. Photobiol.* 82 (2006) 71–77.
- [30] G. Lente, J.H. Espenson, *J. Photochem. Photobiol. A* 163 (2004) 249–258.
- [31] I. Amada, M. Yamaji, S. Tsunoda, H. Shizuka, *J. Photochem. Photobiol. A* 95 (1996) 27–32.
- [32] R.J. Field, E. Körös, R.M. Noyes, *J. Am. Chem. Soc.* 94 (1972) 8649–8664.
- [33] I. Szalai, E. Körös, *J. Phys. Chem. A* 102 (1998) 6892–6897.
- [34] Z. Ungvári-Nagy, I. Zimányi, *React. Kinet. Catal. Lett.* 31 (1986) 249–257.
- [35] K. Pelle, M. Wittmann, Z. Noszticzius, R. Lombardo, C. Sbriziolo, M.L. Turco Liveri, *J. Phys. Chem. A* 107 (2003) 2039–2047.
- [36] J. Horváth, Z. Ungvári-Nagy, S.C. Müller, *Phys. Chem. Chem. Phys.* 3 (2001) 218–223.
- [37] E. Breitmaier, W. Voelter, *Carbon-13 NMR Spectroscopy*, VCH, Würzburg, 1987.
- [38] A. Sirimungkala, H.D. Försterling, V. Diask, R.J. Field, *J. Phys. Chem. A* 103 (1999) 1038–1043.
- [39] E. Chikwana, A. Otoikhian, R.H. Simoyi, *J. Phys. Chem. A* 108 (2004) 11591–11599.
- [40] S. Kawanishi, M. Murata, *Toxicology* 221 (2006) 172–178.
- [41] M. Orban, E. Körös, R.M. Noyes, *J. Phys. Chem.* 83 (1979) 3056–3057.
- [42] P. Herbine, R.J. Field, *J. Phys. Chem.* 84 (1980) 1330–1333.
- [43] P. Sukhai, R.A. McClelland, *J. Chem. Soc., Perkin Trans. 2* (1996) 1529–1530.